Peptide Specificity of Protein Prenyltransferases Is Determined Mainly by Reactivity Rather than Binding Affinity†

Heather L. Hartman,‡,§ Katherine A. Hicks,‡,|| and Carol A. Fierke*,§,||

Departments of Chemistry and Biological Chemistry, University of Michigan, Ann Arbor, Michigan 48109

Received May 23, 2005; Revised Manuscript Received September 13, 2005

ABSTRACT: Protein farnesyltransferase (FTase) and protein geranylgeranyltransferase type I (GGTase I) catalyze the attachment of lipid groups from farnesyl diphosphate and geranylgeranyl diphosphate, respectively, to a cysteine near the C-terminus of protein substrates. FTase and GGTase I modify several important signaling and regulatory proteins with C-terminal CaaX sequences ("C" refers to the cysteine residue that becomes prenylated, "a" refers to any aliphatic amino acid, and "X" refers to any amino acid). In the CaaX paradigm, the C-terminal X-residue of the protein/peptide confers specificity for FTase or GGTase I. However, some proteins, such as K-Ras, RhoB, and TC21, are substrates for both FTase and GGTase I. Here we demonstrate that the C-terminal amino acid affects the binding affinity of K-Ras4B-derived hexapeptides (TKCVIX) to FTase and GGTase I modestly. In contrast, reactivity, as indicated by transient and steady-state kinetics, varies significantly and correlates with hydrophobicity, volume, and structure of the C-terminal amino acid. The reactivity of FTase decreases as the hydrophobicity of the C-terminal amino acid increases whereas the reactivity of GGTase I increases with the hydrophobicity of the X-group. Therefore, the hydrophobicity, as well as the structure of the X-group, determines whether peptides are specific for farnesylation, geranylgeranylation, or dual prenylation.

Protein farnesyltransferase (FTase),[1] protein geranylgeranyltransferase type I (GGTase I), and protein geranylgeranyltransferase type II (GGTase II) comprise the class of enzymes known as the protein prenyltransferases (for review see refs *1* and *2*). Protein prenylation is a type of posttranslational modification in which a 15-carbon farnesyl group from farnesyl diphosphate (FPP) or a 20-carbon geranylgeranyl group from geranylgeranyl diphosphate (GGPP) is covalently attached to a cysteine residue near the C-terminus of the protein substrate (*1*, *2*). The attached lipid enhances membrane association and protein−protein interactions that are necessary for proper functioning of the modified protein (*3*, *4*).

The protein prenyltransferases catalyze thioether bond formation by means of a catalytically essential zinc ion (*1*, *2*, *5*−*7*), which coordinates the cysteine sulfur near the C-terminus of the protein substrate, stabilizing the nucleophilic thiolate (*8*). The Zn(II)-stabilized thiolate nucleophile reacts with the carbon-1 of FPP via a proposed concerted transition state with dissociative character where the peptide thiolate and the bridging oxygen of FPP both bear partial negative charges and the carbon-1 of FPP bears a partial positive charge (*9*). The role of the zinc ion in GGTase I is proposed to be similar to that in FTase (*2*). When both substrates are bound to the enzyme in inactive ternary FTase·FPP·peptide or GGTase I·analogue·peptide complexes, the two reacting atoms, the carbon-1 of FPP/GGPP and the cysteine sulfur of the protein substrate, are over 7 Å apart (*10*, *11*). Kinetic and crystallographic data support the formation of an active substrate conformation prior to catalysis where the carbon-1 of FPP/GGPP moves toward the Zn(II)-bound thiolate to react and the position of the diphosphate alters (*10*−*12*). In FTase and GGTase II, a magnesium ion is required for maximal catalytic activity and is proposed to coordinate the diphosphate of FPP, stabilizing negative charge accumulation on the diphosphate group (*5*, *7*, *9*, *13*, *14*). In GGTase I, the catalytic function of Mg(II) is partially replaced by residue Lys-β311 (*15*).

Prenylated proteins carry out important roles in cellular signaling and regulation that occur at or near cellular membranes. Interestingly, FTase inhibitors (FTIs) show

† This work was supported by National Institutes of Health Grant GM40602 (C.A.F.). Partial funding was also provided by Gaining Assistance in Areas of National Need Grant 037733 (H.L.H.), NIH Training Grant GM07767 NIGMS (H.L.H.), and NIH Training Grant T32 GM08353 (K.A.H.).

* To whom correspondence should be addressed. Phone: (734) 936-2678. Fax: (734) 647-4865. E-mail: fierke@umich.edu.

‡ These authors contributed equally to this work.

§ Department of Chemistry, University of Michigan.

|| Department of Biological Chemistry, University of Michigan.

[1] Abbreviations: FTase, protein farnesyltransferase; GGTase I and II, protein geranylgeranyltransferase types I and II; FPP, farnesyl diphosphate; GGPP, geranylgeranyl diphosphate; FTI, protein farnesyltransferase inhibitor; GGTI, protein geranylgeranyltransferase type I inhibitor; I2, (*E*,*E*)-[2-oxo-2-[[(3,7,11-trimethyl-2,6,10-dodecatrienyl)-oxy]amino]ethyl]phosphonic acid sodium salt; CaaX, tetrapeptide sequence cysteine−aliphatic amino acid−aliphatic amino acid−X (serine, glutamine, or methionine for FTase; leucine or phenylalanine for GGTase I); [^{3}H]FPP, tritium-labeled farnesyl diphosphate; [^{3}H]-GGPP, tritium-labeled geranylgeranyl diphosphate; dns, dansylated; HPLC, high-pressure liquid chromatography; TLC, thin-layer chromatography; Hepes, 4-(2-hydroxyethyl)-1-piperazineethanesulfonic acid; TCEP, tris(2-carboxyethyl)phosphine hydrochloride; Heppso, *N*-(2-hydroxyethyl)piperazine-*N*′-(hydroxypropanesulfonic acid); SDS−PAGE, sodium dodecyl sulfate−polyacrylamide gel electrophoresis; FRET, fluorescence resonance energy transfer; EDTA, (ethylenedinitrilo)tetraacetic acid; MDCC, *N*-[2-(1-maleimidyl)ethyl]-7-(diethylamino)coumarin-3-carboxamide; PP$_i$ase, inorganic pyrophosphatase.

10.1021/bi0509503 CCC: $30.25
Published on Web 10/29/2005

limited toxicity in developed cells, perhaps due to dual prenylation of some protein substrates by both FTase and GGTase I (*17*). Prenylation of Ras oncoproteins is required for membrane association and subsequent oncogenic activity, identifying FTIs and GGTase I inhibitors (GGTIs) as targets for cancer therapy (*2*, *18*). Given the biological and clinical importance of prenylation, it is important to understand the in vivo substrate specificity of these enzymes. FTase and GGTase I have been proposed to prenylate proteins or peptides with C-terminal CaaX sequences where "C" refers to the cysteine residue that becomes prenylated, "a" refers to any aliphatic amino acid, and "X" refers to methionine, serine, glutamine, or alanine for FTase and leucine or phenylalanine for GGTase I (*19*−*24*). In the CaaX paradigm, the C-terminal X-residue confers the specificity of the protein or peptide for FTase or GGTase I (*19*−*24*). However, some proteins, such as K-Ras4B, have been shown to be substrates for both FTase and GGTase I, indicating that the specificity of these enzymes may be broader than the CaaX paradigm predicts (*25*, *26*).

Structurally, FTase and GGTase I are α/*β* heterodimers with identical α-subunits and *β*-subunits with only 25% identity (*2*, *11*). Thus, the differential CaaX substrate preferences of these enzymes are due to differences in their *β*-subunits. In the crystal structures of ternary complexes of FTase [FTase·FPT inhibitor II (I2)·TKCVIM] and GGTase I [GGTase I·3-aza-GGPP·TKCVIL], the carboxylate of the protein/peptide X-residue forms a hydrogen bond with the side chain of residue Gln167α and a buried solvent molecule, which, in turn, is coordinated by Glu198*β*, His149*β*, and Arg202*β* of FTase (Glu169*β*, His121*β*, and Arg173*β* in GGTase I) (*11*, *27*). In the crystal structure of FTase complexed with I2 and KKKSKTKCVIM, the C-terminal methionine side chain forms van der Waals contacts with Ala98*β*, Ser99*β*, Trp102*β*, His149*β*, Ala151*β*, Pro152*β*, and Tyr131α (*27*) (Figure 1A). However, in the crystal structure of the GGTaseI·3-aza-GGPP·KKSKTKCVIL complex, the van der Waals contacts with Leu are altered; Thr45*β*, Thr49*β*, and Met124*β* in GGTase replace Ala98*β*, Trp102*β*, and Pro152*β*, respectively, in FTase (Figure 1) (*11*, *27*).

Here we examine features of the C-terminal amino acid that are important for determining the substrate specificity of FTase and GGTase I. To do this, we measured the affinity and reactivity of FTase and GGTase I with a series of peptides using a K-Ras4B-derived hexapeptide template (TKCVIM) with various C-terminal X-residues (TKCVIX). We chose K-Ras4B as our template since this is the form of Ras most often mutated in human cancers and it is prenylated by both FTase and GGTase I. As such, K-Ras4B defies the traditional "CaaX" paradigm and is largely resistant to inhibition of prenylation by FTIs due to prenylation catalyzed by GGTase I (*25*). We demonstrate that the peptide specificity of these enzymes is determined mainly by changes in reactivity, as measured by both transient and steady-state kinetics, which generally correlate with the hydrophobicity of the C-terminal amino acid. These data not only broaden our understanding of the definition of FTase and GGTase I substrate specificity but also outline the kinetic and thermodynamic contributions of the enzyme binding pockets to specificity and cross-reactivity (*25*−*26*).

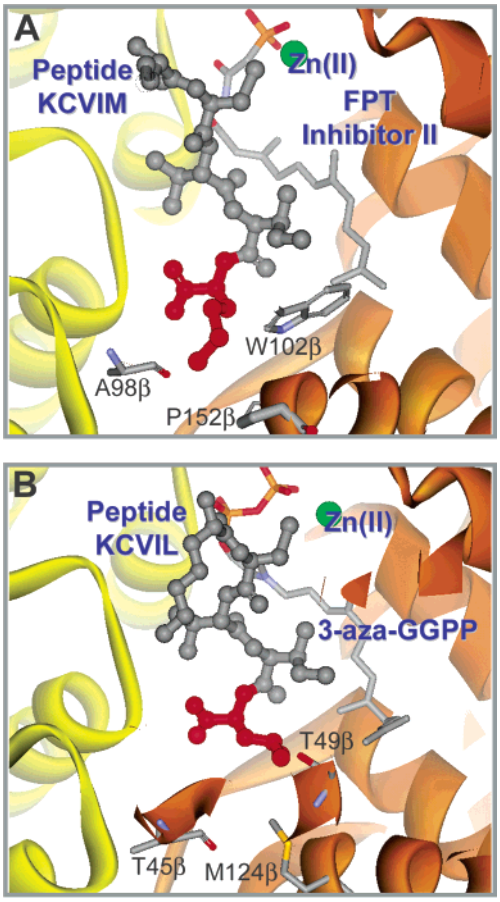

FIGURE 1: Peptide binding sites of wild-type FTase and GGTase I. The C-terminal X-residues of the peptide substrates (methionine and leucine, respectively) appear in red, the α-subunits in yellow, and the *β*-subunits in orange. Figures were generated from Protein Data Bank files using ViewerPro (Accelrys Software Inc., San Diego, CA) and Photoshop (Adobe Systems Inc., San Jose, CA) software. Panel A: Crystallographic model of the FTase specificity pocket with bound I2 and K-Ras4B peptide (Protein Data Bank code 1D8D) (*27*). Panel B: Crystallographic model of the GGTase I specificity pocket with bound 3-aza-GGPP and peptide KKSK-TKCVIL (Protein Data Bank code 1N4Q) (*11*).

EXPERIMENTAL PROCEDURES

Miscellaneous Methods. All assays were performed at 25 °C. All curve fitting was performed with Kaleidagraph (Synergy Software, Reading, PA). Tritium-labeled farnesyl diphosphate ([^{3}H]FPP) and geranylgeranyl diphosphate ([^{3}H]-GGPP) were purchased from Amersham Biosciences (Piscataway, NJ). Peptides were synthesized and purified by high-pressure liquid chromatography as follows: dansylated GCVLL (dns-GCVLL), TKCVIS, dns-TKCVIM, and TKCVIM by Bethyl Laboratories (Montgomery, TX); TKCVIQ, TKCVIF, TKCVIL, and TKCVIN by American Peptide Co. (Sunnyvale, CA), and peptides TKCVIX (where X = A, I, Y, and N) and dns-TKCVIX (where X = A, C, D, F, I, L, M, N, Q, R, S, T, V, and Y) by Sigma-Genosys (The Woodlands, TX). Peptide purities were ≥70% as indicated by mass spectrometry; the major contaminants are smaller peptide fragments. The concentration of each peptide was determined spectroscopically at 412 nm by reaction of the cysteine thiol with 5,5′-dithiobis(2-nitrobenzoic acid), using an extinction coefficient of 14150 M^{-1} cm^{-1} (*28*). Inorganic pyrophosphatase from bakers' yeast, 7-methylguanosine, and purine nucleoside phosphorylase were purchased

from Sigma (St. Louis, MO). All other chemicals were of reagent grade. Thin-layer chromatography (TLC) plates were prerun in 100% acetone before use.

Preparation of FTase and GGTase I. Wild-type FTase was expressed in BL21(DE3) FPT/pET23a *Escherichia coli* and purified as described previously (*14*, *29*). FTase concentration was determined by active site titration (*14*). The purified FTase was determined by SDS−PAGE to be >90% pure. The protein was dialyzed against HT buffer [50 mM 4-(2-hydroxyethyl)-1-piperazineethanesulfonic acid (Hepes), pH 7.8, 1 mM tris(2-carboxyethyl)phosphine hydrochloride (TCEP)], concentrated to 270 μM, and frozen at −80 °C.

Wild-type GGTase I was expressed in BL21(DE3) GGPT/pET23a *E. coli* and purified as described previously except that the second Poros HQ column (Applied Biosystems, 7.9 mL bed volume) was omitted (*15*). The purified GGTase I was determined by SDS−PAGE to be >90% pure. The protein was dialyzed against HT buffer, concentrated to 95 μM, and frozen at −80 °C. GGTase I concentration was determined by active site titration of GGTase I with dns-GCVLL (*8*). The binding of dns-GCVLL to GGTase I was observed by fluorescence resonance energy transfer (FRET) whereby the tryptophan residues of GGTase I are excited at 280 nm, and their emission at 340 nm, in turn, excites the bound dansyl group whose emission is monitored at 490 nm. The assay was performed in 96-well plate format where each well contained 50 mM Heppso, pH 7.8, 2 mM TCEP, ∼500 nM GGTase I, and 0−1 μM dns-GCVLL. The plate was incubated with shaking for 5 min prior to measurement in a PolarStar Galaxy platereader (BMG Labtechnologies, Durham, NC). Lines were fit separately to the first 10% of the binding titration and to the points >500 nM. The intersection point of the two lines, representing formation of a 1:1 GGTase I·dns-GCVLL complex, was used to determine the concentration of GGTase I in the sample.

Peptide Binding Affinities. The affinities of FTase·I2 and GGTase I·3-aza-GGPP (*30*) (a gift from Robert Coates, University of Illinois) for the dansylated peptide substrates were determined by fluorescence anisotropy as described previously (*15*). In this method, the dansyl group of the peptide is excited at 340 nm (band-pass = 16 nm), and its emission is monitored at 496 nm (FTase, band-pass = 16 nm) or 525 nm (GGTase I, band-pass = 16 nm). FTase and GGTase I samples were prepared with 50 mM Heppso, pH 7.8, 2 mM TCEP, 10 nM (ethylenedinitrilo)tetraacetic acid (EDTA), and 2 nM dns-TKCVIX and then titrated with either FTase·I2 or GGTase I·3-aza-GGPP (0−500 nM). For FTase, 5 mM $MgCl_2$ was included. The samples were incubated for 5 min prior to each measurement at 25 °C. A weighted fit of eq 1 to the data yields the apparent dissociation constants, where ΔA corresponds to the observed fluorescence anisotropy, EP is the fluorescence anisotropy end point, IF is the initial fluorescence anisotropy, [enzyme] is the concentration of FTase or GGTase I, and $K_D^{peptide}$ is the dissociation constant for dns-TKCVIX.

$$\Delta A = \frac{EP}{1 + K_D^{peptide}/[enzyme]} + IF \quad (1)$$

Competition Peptide Binding Affinity. The affinity of FTase for the unlabeled peptide TKCVID was determined as previously described by measuring competition with dns-GCVLS (*8*). The FTase·I2·dns-GCVLS complex was observed by FRET (excitation at 280 nm and emission at 496 nm). The formation of FTase·I2·unlabeled peptide complex was observed by a decrease in FRET in 50 mM Heppso, pH 7.8, 2 mM TCEP, 1 mM $MgCl_2$, 20 nM FTase, 40 nM I2, 40 nM dns-GCVLS, and 10 nM EDTA; ionic strength was maintained at 0.1 M with the addition of NaCl. The samples were titrated with TKCVID (0−3 μM). A fit of eq 2 to the data yielded the apparent dissociation constants, where ΔFL is the observed fluorescence at 496 nm corrected for background, IF is the initial fluorescence, EP is the fluorescence end point, $K_D^{peptide}$ is the dissociation constant for the dansylated peptide, [peptide] is the concentration of the dansylated peptide, [unlabeled] is the concentration of the unlabeled peptide, and $K_D^{unlabeled}$ is the dissociation constant of the unlabeled peptide.

$$\Delta FL = \frac{IF}{1 + (K_D^{peptide}/[peptide])(1 + [unlabeled]/K_D^{unlabeled})} + EP \quad (2)$$

Transient Kinetics. Single turnover assays were performed for wild-type FTase and GGTase I in 50 mM Heppso, pH 7.8, and 2 mM TCEP as described previously (*13*, *15*). For FTase, 5 mM $MgCl_2$ was included in the reaction buffer. Reactions with prenylation rate constants less than 0.1 s^{-1} were performed manually using 0.8−1.0 μM enzyme, 0.4 μM [^{3}H]FPP or [^{3}H]GGPP, and 50−800 μM peptide. The enzyme was preincubated with [^{3}H]FPP or [^{3}H]GGPP for 15 min at room temperature. The reactions were initiated by addition of saturating peptide and quenched at varying times (3 s to 4 h) by the addition of an equal volume of cold 80% 2-propanol and 20% acetic acid (v/v). For reactions with rate constants faster than 0.1 s^{-1}, a KinTek rapid quench apparatus was used (KinTek Corp., Austin, TX). The reactions contained 0.8−1.0 μM enzyme, 0.4 μM [^{3}H]FPP or [^{3}H]GGPP, and 50−800 μM peptide and were quenched with 80% 2-propanol and 20% acetic acid at varying times (0.005−120 s), then dried under vacuum, and resuspended in 50% 2-propanol. The product was separated from substrate by TLC on silica gel plates (Whatman PE SIL G) with an 8:1:1 (v/v/v) 2-propanol/NH_4OH/H_2O mobile phase. The product migrates in this mobile phase, but the FPP and GGPP substrates remain at the origin; the plates were cut accordingly, and the radioactivity was quantified by scintillation counting. The radioactivity in the product was divided by the total radioactivity for each time point to calculate the fraction of product formed. The rate constant for product formation (k_{obs}) was determined by fitting eq 3 to the data, where P_t is the fraction product formed at time t and P_∞ is the calculated reaction end point, which varied from 60% to 90%.

$$P_t/P_\infty = 1 - e^{-k_{obs}t} \quad (3)$$

Alternatively, single turnover assays were performed for FTase and GGTase I in 50 mM Heppso, pH 7.8, 5 mM $MgCl_2$, and 2 mM TCEP in the presence of *N*-[2-(1-maleimidyl)ethyl]-7-(diethylamino)coumarin-3-carboxamide-labeled phosphate binding protein (MDCC-labeled PBP) (*31*) and inorganic pyrophosphatase (PP_iase) to measure formation

of diphosphate (*32*). MDCC-labeled PBP was dialyzed against 0.5 unit μL^{-1} purine nucleoside phosphorylase and 15 μM 7-methylguanosine to form ribose 1-phosphate from any monophosphate contaminants. FTase and GGTase I were preincubated with FPP and GGPP, respectively, for 15 min at room temperature; the reactions were initiated by addition of dns-TKCVIX, MDCC-labeled PBP, and PP_iase. The final concentrations were 0.8 μM FTase or GGTase I, 0.2 μM FPP or GGPP, 100 μM dns-TKCVIX, 5 μM MDCC-labeled PBP (*31*), and 33 units mL^{-1} PP_iase. A KinTek stopped-flow instrument (KinTek Corp., Austin, TX) was used to monitor the binding of inorganic phosphate to the MDCC-labeled PBP, which is observed as an increase in fluorescence (λ_{ex} = 430 nm cutoff filter, λ_{em} = 450 nm cutoff filter). Under these conditions, the rate of cleavage of the pyrophosphate product catalyzed by PP_iase and the association rate for phosphate binding to MDCC-labeled PBP are fast relative to the rate constant for diphosphate formation and release catalyzed by the prenyltransferases (>10-fold) (*32*). The rate constant for product formation (k_{chem}) was determined by fitting eq 3 to the fluorescence change as a function of time, where P_t is the fraction product formed at time t as indicated by fluorescence and P_∞ is the reaction end point (the maximal change in fluorescence).

Steady-State Kinetics. The steady-state kinetics were determined for FTase using a radioactive assay as previously described (*14*). The final concentrations were 24 nM FTase, 1 μM [^{3}H]-FPP, and 0.1−10 μM peptide in 50 mM Heppso-NaOH, pH 7.8, 5 mM $MgCl_2$, and 2 mM TCEP. Reactions were quenched by the addition of an equal volume of 20% (v/v) acetic acid/80% 2-propanol, and product was measured by TLC, as described.

The steady-state kinetics were measured for GGTase I from the time-dependent increase in fluorescence intensity (λ_{ex} = 340 nm, λ_{em} = 520 nm) upon prenylation of dns-TKCVIX. Assays were performed at 25 °C in 0.1−10 μM dns-TKCVIX, 10 μM GGPP, 50 mM Tris-HCl, pH 7.5, 5 mM DTT, 5 mM $MgCl_2$, and 10 μM $ZnCl_2$ in a 96-well plate (*33*). Reactions were initiated by the addition of GGTase I (25−100 nM), which was at least 3-fold lower than the concentration of peptide. The fluorescence intensity was measured every 2 min until the end point was reached. The linear, initial rate (<10% of the total reaction) in fluorescence intensity per second was converted to the rate of increase in concentration of product per second using eq 4, where V refers to the velocity of the reaction in micromolar per second, R refers to the velocity of the reaction in fluorescence units per second, P refers to the concentration of the limiting substrate, and F_{max} refers to the maximal fluorescence intensity at the end point (*35*).

$$V = RP/F_{max} \quad (4)$$

The steady-state kinetic parameters, k_{cat} and $k_{cat}/K_M^{peptide}$, are generally determined from a fit of the Michaelis−Menten equation to the dependence of the initial rate divided by the concentration of enzyme on the peptide concentration at saturating FPP/GGPP. However, in the interest of designing a high-throughput screen, the value of k_{cat}/K_M was determined from the linear dependence of the initial velocity on subsaturating peptide concentrations. A lower limit for k_{cat} was estimated by measuring the steady-state turnover rate at 10 μM peptide, significantly higher than measured values of $K_M^{peptide}$ (*33*), assuming that the peptide is saturating at this concentration so that V reflects V_{max}. This is a reasonable assumption for all of the peptides except TKCVID, where $K_D^{peptide}$ is very high for FTase.

RESULTS

K-Ras4B Peptide Template. Short peptides encompassing the CaaX sequence can compete with full-length proteins for farnesylation, and structurally, the CaaX sequence appears to be the primary recognition element for both FTase and GGTase I (*11*, *20*, *36*−*38*). Previous steady-state kinetic studies of the substrate specificity of rat FTase and GGTase I suggest that the identity of the C-terminal residue of the protein substrate is a main determinant of specificity (*19*−*24*). Sequence alignments and crystallographic analyses of FTase and GGTase I support these data as they reveal variability in the binding sites for the side chain of the C-terminal residue of the peptide substrate (*11*, *27*, *36*). In fact, crystallographic studies of FTase in complex with FPT inhibitor II and various peptide sequences suggest multiple conformations of the X-group side chain that may correlate with reactivity (36). However, no systematic study of the effect of varying the X-residue on the affinity and reactivity of the peptide has yet been carried out. To examine the importance of the X-residue, we measured the peptide affinity and reactivity with FTase and GGTase I using a peptide template corresponding to the C-terminus of the protein K-Ras4B (TKCVIM) where the terminal methionine is substituted with one of the following amino acids: Ala, Cys, Asp, Phe, Ile, Leu, Asn, Gln, Arg, Ser, Thr, Val, or Tyr.

Substrate Binding Affinity. The binding affinities of the FTase•I2 and GGTase I•3-aza-GGPP complexes, respectively, for dansylated peptide substrates were measured from changes in fluorescence anisotropy (Figure 2). The dissociation constants from the FTase•I2•TKCVIX complex are between 6 and 26 nM for the majority (10 out of 14) of the substituted amino acids (Table 1), indicating that peptide affinity is not the main determinant of specificity in FTase. However, three peptides have higher affinity (TKCVIM, TKCVIF, and TKCVIL with K_D values of ~1 nM, Table 1) including two of the X-groups that are proposed to confer specificity for GGTase I (F and L), while the one peptide containing a negatively charged X-group, TKCVID, binds significantly less tightly (~1300 nM, Table 1). The weak affinity of FTase•I2 for TKCVID could be due to repulsion of the aspartate side chain of the peptide with FTase residue Glu198β in the specificity pocket, the inability of the aspartate side chain of the peptide to hydrogen bond with H149β, and/or unfavorable hydrophobic van der Waals contacts between the aspartate side chain of the peptide with FTase residues Ala98β, Trp102β, Ala151β, Pro152β, or Tyr131α.

Similarly, the binding affinities of the GGTase I•3-aza-GGPP complex for dns-TKCVIX peptide substrates (Figure 2) are within an order of magnitude (3−40 nM) of one another for all of the substituted amino acids, including Leu and Phe, except for the weakest binding peptide, TKCVIR (110 nM), which contains a positively charged amino acid in the X-position. Unexpectedly, the peptides containing a C-terminal methionine, TKCVIM (3 ± 1 nM), or aspartate,

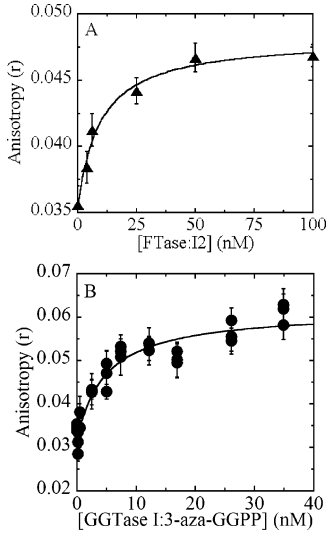

FIGURE 2: Peptide binding affinities for wild-type FTase and GGTase I. Panel A: The dissociation constant for dns-TKCVIQ (▲) for FTase was determined by fluorescence anisotropy (λ_{ex} = 340 nm, λ_{em} = 496 nm) as described under Experimental Procedures. The assay contained 50 mM Heppso, pH 7.8, 2 mM TCEP, 1 mM $MgCl_2$, 10 nM EDTA, and 2 nM dns-TKCVIQ. The samples were titrated with FTase·I2 (0−100 nM). The value of K_D^{TKCVIQ} was determined by a weighted fit of eq 1 to these data. Panel B: The dissociation constant for dns-TKCVIM (●) was determined by fluorescence anisotropy (λ_{ex} = 340 nm, λ_{em} = 525 nm). Dns-TKCVIM (2 nM) was preincubated in 50 mM Heppso, pH 7.8, 2 mM TCEP, and 10 nM EDTA at 25 °C and then titrated with GGTase I·3-aza-GGPP (0−40 nM). The value of K_D^{TKCVIM} was determined by a weighted fit of eq 1 to these data.

TKCVID (4 ± 1 nM), bind to GGTase I with the highest affinity. The tight affinity of TKCVID for GGTase I·3-aza-GGPP suggests that the negatively charged aspartate residue either binds in a different position or interacts with different residues in the specificity pocket of GGTase I compared to FTase. Of the van der Waals contacts listed above for FTase, three of five residues are different in GGTase I; Ala98β, Trp102β, and Pro152β in FTase are replaced with Thr45β, Thr49β, and Met 124β in GGTase I. These amino acid substitutions create a more polar specificity pocket in GGTase I, likely yielding a tighter binding affinity for TKCVID. In summary, the similarity in binding affinities for these peptides suggests that the thermodynamics of peptide binding is not the main determinant of substrate specificity of FTase and GGTase I.

Transient Kinetics of FTase and GGTase I. The rate constants for prenylation of TKCVIX catalyzed by FTase and GGTase I were determined under single turnover conditions, where the enzyme and peptide concentrations are in excess of the prenyl diphosphate concentration. Previous kinetic data suggest the basic kinetic scheme illustrated in Scheme 1 for both FTase and GGTase I, where substrate binding is functionally ordered with FPP/GGPP binding before peptide and the rate constant for prenylation is faster than product dissociation (*9*, *39*−*42*). For both enzymes, the single turnover rate constant measures the formation of the E·product complex from the E·FPP/GGPP·peptide ternary complex and likely reflects the rate constant for prenylation catalyzed by FTase and GGTase I (*9*, *15*).

For FTase, the single turnover rate constants for farnesylation of TKCVIX vary by more than 7000-fold where TKCVIM (7.3 ± 0.7 s^{-1}) and TKCVIS (6 ± 1 s^{-1}) have the fastest prenylation rate constants (Figure 3, Table 1) and TKCVIR, containing a positively charged side chain, has the slowest prenylation rate constant (<0.001 s^{-1}, Table 1). In general, FTase is most efficient at catalyzing farnesylation of peptide substrates possessing small, polar X-groups. For example, in the following series the prenylation rate constant increases as the hydrophobicity of the side chain of the X-group decreases: V (0.66 ± 0.06 s^{-1}) < A (1.8 ± 0.8 s^{-1}) < T (2.4 ± 0.2 s^{-1}) < S (6 ± 1 s^{-1}).

For GGTase I, the single turnover rate constants for prenylation of TKCVIX vary by more than 900-fold (Table 2). Peptides with nonpolar X-groups (TKCVIV, TKCVIL, and TKCVIF) have the fastest geranylgeranylation rate constants (0.7−0.9 s^{-1}), which are 2−3-fold faster than reaction with TKCVIM (0.35 ± 0.02 s^{-1}, Figure 3, Table 2) but ∼10-fold slower than the maximal rate constants observed for farnesylation catalyzed by FTase (Table 1). The peptides with charged X-groups, TKCVID and TKCVIR, have the slowest prenylation rate constants (<0.001 s^{-1}, Table 2). In contrast to FTase, GGTase I is most efficient at prenylating peptide substrates possessing nonpolar X-groups. For example, in the following series of X-groups, the prenylation rate constant decreases as the hydrophobicity of the side chain decreases: V (0.91 ± 0.09 s^{-1}) > T (0.19 ± 0.01 s^{-1}) > S (0.028 ± 0.002 s^{-1}). These data demonstrate that the reactivity of the peptides bound to FTase and GGTase I is sensitive to the structure, size, and hydrophobicity of the X-group. Importantly, the peptide specificities of FTase and GGTase I are mainly determined by reactivity and not affinity. Furthermore, the differential specificity of FTase and GGTase I for the C-terminal X-group is affected by differential sensitivity to the hydrophobicity of this group.

Effect of Alterations of the X-Residue of the Peptide Substrate on Steady-State Turnover. To further investigate the importance of the X-group for substrate specificity, the steady-state parameters k_{cat} and k_{cat}/K_M were measured using either a radioactive assay or continuous fluorescence assay with dansylated peptide substrates (Tables 1 and 2). The kinetic parameter k_{cat}/K_M is termed the "specificity constant" (*43*) and should indicate the relative reactivity of the enzyme with different peptides. The values of k_{cat}/K_M vary by >40-fold for GGTase I and by >900-fold for FTase, indicating that the X-group of the peptide substrate is a major determinant of substrate selectivity (Tables 1 and 2). These data demonstrate that FTase is most selective for catalyzing prenylation of TKCVIM, TKCVIQ, TKCVIC, and TKCVIS ($k_{cat}/K_M > 10^4$ M^{-1} s^{-1}, Table 1) followed by TKCVIA, TKCVIN, and TKCVIT ($k_{cat}/K_M > 10^3$ $M^{-1}s^{-1}$, Table 1). This list includes the X-groups (M, S, Q, and A) previously observed most frequently in FTase substrates (*2*). However, steady-state turnover is also observed for peptides containing a variety of other X-groups (D, F, V, and Y). Conversely, GGTase I is most specific for reacting with TKCVIF, TKCVII, TKCVIL, and TKCVIM ($k_{cat}/K_M > 10^4$ M^{-1} s^{-1}, Table 2) with decreased specificity for TKCVIC, TKCVIV, and TKCVIY ($k_{cat}/K_M > 10^3$ M^{-1} s^{-1}, Table 2). These data also indicate that the peptides with nonpolar X-groups are the preferred substrates for GGTase I and that the peptides with polar X-groups are the preferred substrates for FTase.

For both FTase and GGTase I, the steady-state rate constant k_{cat} is proposed to reflect the rate constant for

Table 1: Kinetic and Thermodynamic Constants of Wild-Type FTase

peptide	$K_D^{peptide}$ (nM)[a]	k_{chem} (s^{-1})[b]	k_{cat} (s^{-1})[c]	k_{cat}/K_M (M^{-1} s^{-1})[c]
TKCVIA	18 ± 5	1.8 ± 0.8	0.046 ± 0.002	3700 ± 200
TKCVIC	7 ± 1	3.2 ± 0.3	0.31 ± 0.02	35000 ± 2000
TKCVID	1300 ± 200[d]	0.33 ± 0.03	0.00050 ± 0.00006	80 ± 30
TKCVIF	1.1 ± 0.1	0.06 ± 0.01	0.0082 ± 0.0008	900 ± 60
TKCVII	16 ± 4	0.14 ± 0.02	<0.001[e]	<100[f]
TKCVIL	1.1 ± 0.1	0.07 ± 0.01	<0.001[e]	<100[f]
TKCVIM	0.86 ± 0.08	7.3 ± 0.7	0.041 ± 0.004	16000 ± 1000
TKCVIN	15 ± 3	1.8 ± 0.1	0.013 ± 0.001	1500 ± 100
TKCVIQ	12 ± 5	2.4 ± 0.8	0.161 ± 0.006	44000 ± 2000
TKCVIR	7 ± 2	<0.0001[g]	<0.001[e]	<100[f]
TKCVIS	26 ± 5	6 ± 1	0.21 ± 0.02	14200 ± 600
TKCVIT	8 ± 2	2.4 ± 0.2	0.017 ± 0.001	1000 ± 30
TKCVIV	7 ± 2	0.66 ± 0.06	0.0021 ± 0.0004	60 ± 10
TKCVIY	6 ± 1	0.12 ± 0.02	0.0017 ± 0.0002	100 ± 10

[a] Peptide dissociation constants were measured with dansylated peptides at pH 7.8. [b] k_{chem} is the single turnover rate constant for product formation at pH 7.8 at 5 mM $MgCl_2$. [c] The steady-state kinetics were determined at saturating concentrations of FPP (10 μM) and varying TKCVIX (0.1−10 μM) in 24 nM FTase, 50 mM Heppso, pH 7.8, 5 mM $MgCl_2$, and 2 mM TCEP. The value of k_{cat} was estimated at saturating (10 μM) peptide.[d] The peptide dissociation constant was measured with unlabeled peptide by competition with dns-GCVLS at pH 7.8. [e] Less than 10% product was formed in 4 h so that the k_{chem} was <0.0001 s^{-1}, assuming an end point of 100%. [f] Less than 10% product was formed in 1 h so that the initial rate was <0.001 s^{-1}, assuming an end point of 100%. [g] Less than 10% product was formed in 1 h so that the maximal k_{cat}/K_M was <100 M^{-1} s^{-1}, assuming K_M > [peptide].

Scheme 1: Kinetic Mechanism for FTase[a]

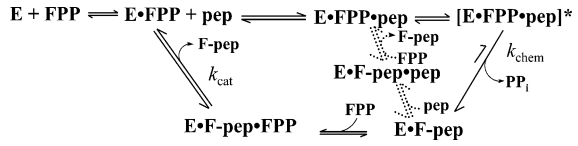

[a] For GGTase I, FPP is replaced by GGPP.

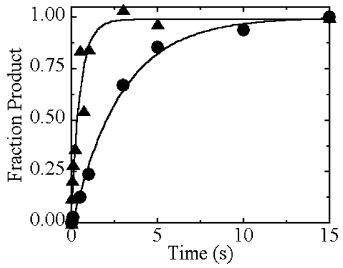

FIGURE 3: Single turnover kinetics for FTase and GGTase I with TKCVIM. Single turnover rate constants were measured as described under Experimental Procedures. Assays contained 0.8−1.0 μM FTase (▲) or GGTase I (●), 0.4 μM [^{3}H]FPP or [^{3}H]GGPP, saturating peptide (51−800 μM), 50 mM Heppso, pH 7.8, and 2 mM TCEP. For FTase reactions, 5 mM $MgCl_2$ was added to the reaction buffer, and the ionic strength was maintained at 0.2 M with NaCl. The data were normalized for clarity using the formula (fraction of product − background)/(fraction of $product_{max}$ − background). The prenylation rate constant k_{chem} was calculated by a fit of eq 3 to the data.

product dissociation (*42*, *44*) so this kinetic constant can be used to evaluate the importance of the X-group for product dissociation. For the majority of the TKCVIX peptides, the single turnover prenylation rate constant is faster than k_{cat} (Tables 1 and 2), suggesting that product dissociation remains the rate-limiting step in k_{cat}. For FTase, the values of k_{cat} vary by >300-fold, where product dissociation is fastest for TKCVIC, TKCVIS, and TKCVIQ (k_{cat} > 0.1 s^{-1}, Table 1) and slowest for TKCVII and TKCVIL (k_{cat} < 0.001 s^{-1}, Table 1). These data suggest that the identity of the X-residue also affects the rate constant for product dissociation with peptides containing a polar X-residue dissociating more rapidly from FTase than substrates with nonpolar X-residues. The structure of the X-residue has a larger effect on the product dissociation rate constant than on the substrate affinity, suggesting differential interactions with the protein in the two complexes. The measurable values of k_{cat} for GGTase I are less variable; omitting TKCVIC, the values of k_{cat} vary only 5-fold for nonpolar X-groups (F, I, L, M, V, and Y). However, no steady-state turnover is observable for peptides containing a polar X-group (N, Q, S, and T), suggesting that product dissociation is very slow. Therefore, nonpolar X-groups enhance the rate constant for product dissociation from GGTase I. These data demonstrate that the X-group modulates the rate constants for both prenylation and product dissociation. In general, the rate constants for FTase are enhanced by polar X-groups while those for GGTase I are increased by nonpolar groups.

A significant fraction of the peptides examined did not exhibit any measurable steady-state turnover activity. Thus, the peptides can be divided into three classes: (A) those that bind but do not react (X = D and R for GGTase I; X = R for FTase), (B) those that bind and catalyze a single turnover but not multiple turnovers (X = A, N, Q, S, and T for GGTase I; X = I and L for FTase), and (C) those that bind and react under both single and multiple turnover conditions (X = C, F, I, L, M, V, and Y for GGTase I; X = A, C, D, F, M, N, Q, S, T, V, and Y for FTase). Classes A and C were expected. However, we were surprised to observe peptides that bind to these enzymes and form product in a single turnover but do not have multiple turnover activity (class B). These data suggest that the prenylated products of these peptides do not dissociate readily from the enzyme, an extreme case of product inhibition. One possible explanation for the class B peptides is that the X-group of the prenylated peptide forms highly favorable interactions with the binding pocket of FTase or GGTase I that significantly enhance the affinity of the product to prevent product dissociation. Alternatively, upon prenylation of the peptide, the X-group could adopt a conformation in the active site that kinetically blocks dissociation, perhaps by hindering either movement of the prenylated product into the exit groove or binding of a subsequent molecule of FPP or GGPP (*10*, *11*). The observed lack of steady-state turnover for these

Table 2: Kinetic and Thermodynamic Constants of Wild-Type GGTase I

peptide	$K_D^{peptide}$ (nM)[a]	k_{chem} (s^{-1})[b]	k_{cat} (s^{-1})[c]	k_{cat}/K_M (M^{-1} s^{-1})[c]
TKCVIA	17 ± 3	0.015 ± 0.004	<0.001[e]	<100[f]
TKCVIC	8 ± 1	0.048 ± 0.004	0.0063 ± 0.0004	4000 ± 1000
TKCVID	4 ± 1	<0.0001[d]	<0.001[e]	<100[f]
TKCVIF	20 ± 10	0.7 ± 0.2	0.06 ± 0.01	13000 ± 1000
TKCVII	9 ± 1	0.24 ± 0.02	0.048 ± 0.002	15000 ± 2000
TKCVIL	20 ± 10	0.82 ± 0.09	0.088 ± 0.001	39000 ± 9000
TKCVIM	3 ± 1	0.35 ± 0.02	0.082 ± 0.009	16000 ± 1000
TKCVIN	7 ± 4	0.15 ± 0.02	<0.001[e]	<100[f]
TKCVIQ	9 ± 5	0.031 ± 0.004	<0.001[e]	<100[f]
TKCVIR	110 ± 20	<0.0001[d]	<0.001[e]	<100[f]
TKCVIS	12 ± 6	0.028 ± 0.002	<0.001[e]	<100[f]
TKCVIT	19 ± 9	0.19 ± 0.01	<0.001[e]	<100[f]
TKCVIV	40 ± 10	0.91 ± 0.09	0.107 ± 0.004	1000 ± 600
TKCVIY	14 ± 4	0.054 ± 0.009	0.022 ± 0.001	1600 ± 300

[a] Peptide dissociation constants were measured with dansylated peptides at pH 7.8. [b] k_{chem} is the single turnover rate constant for product formation at pH 7.8 in the absence of $MgCl_2$. [c] The steady-state kinetics were determined at saturating concentrations of GGPP (10 μM) and varying TKCVIX (0.1−10 μM) in 25−100 nM GGTase I, 50 mM Tris-HCl, 5 mM DTT, 5 mM $MgCl_2$, and 10 μM $ZnCl_2$. [d] Less than 10% product was formed in 4 h so that the k_{chem} was <0.0001 s^{-1}, assuming an end point of 100%. [e] Less than 10% product was formed in 1 h so that the k_{cat} was <0.001 s^{-1}, assuming an end point of 100%. [f] Less than 10% product was formed in 1 h so that the k_{cat}/K_M was <100 $M^{-1}s^{-1}$, assuming K_M > [peptide].

class B peptides may be a second mechanism for determining substrate specificity.

However, the class B peptides could potentially be prenylated and released in vivo if other cellular factors enhance product dissociation. This hypothesis is validated by experiments indicating that farnesylated TKCVIL (class B peptide) is *not* an inhibitor of the reaction of FTase with a second peptide, dns-TKCVIC (class C peptide), as would be expected if dissociation of farnesylated TKCVIL from FTase is extremely slow. In these experiments, FTase, FPP, and TKCVIL (1:1:1 stoichiometry) are incubated at 25 °C for 1 h to form the E·F-peptide product. No multiple turnover activity is observed when this complex is diluted 250-fold into an assay containing 10 μM FPP and 1 μM dns-TKCVIL, consistent with the lack of multiple turnover activity previously demonstrated (Table 1). However, when this inactive product complex (E·farnesylated-TKCVIL) is diluted into an assay containing 10 μM FPP and 1 μM active peptide dns-TKCVIC (Table 1), multiple turnover activity is immediately observed. The value of $k_{cat}/K_M^{peptide}$ (35000 M^{-1} s^{-1}) under these conditions is identical to the value measured in the absence of preincubation with TKCVIL/FPP. These experiments suggest that FPP and the peptide dns-TKCVIC catalyze dissociation of the farnesylated TKCVIL product from FTase even though FPP and dns-TKCVIL do not enhance product dissociation. Catalysis of product dissociation from FTase by a peptide has been suggested previously (*45*) although this process has not been as well characterized as the FPP-catalyzed product dissociation. These data suggest that FTase has the potential to catalyze multiple turnovers of farnesylation of TKCVIL in the presence of a second peptide that can enhance product dissociation. Therefore, the loss of FTase-catalyzed multiple turnover of the peptide TKCVIL reflects the inability of FPP alone to catalyze product dissociation. This mechanism is likely to be true for the other class B peptides as well. These data suggest the possibility that farnesylation of one protein can be enhanced by the presence of a second protein substrate, which could function as a novel regulatory mechanism.

Sensitivity of Reactivity to Hydrophobicity and Size of the X-Residue. To further examine the role of the hydrophobicity and/or size of the X-group in determining the reactivity and affinity of peptide substrates, we correlated the $\Delta\Delta G_{dissoc}$[2] for binding affinity and the $\Delta\Delta G^{\ddagger}$[2] for reactivity with either the $\Delta G°_{transfer}$ between octanol and water (Figure 4, $\Delta G°_{transfer}$ taken from ref *46*) or the volume (*46*) of each amino acid side chain located in the X-position. We omitted both the charged C-terminal amino acids and the peptides with k_{cat}/K_M values below the detection limit of the assay from this analysis.

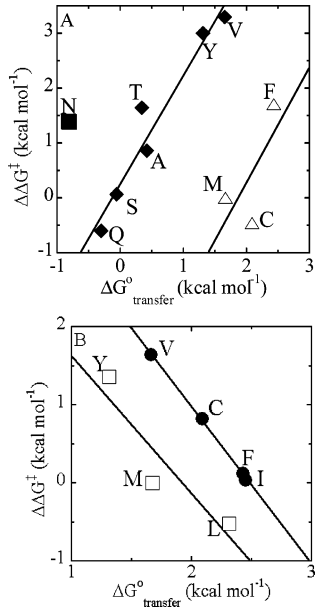

FIGURE 4: Comparison of kinetic data for FTase (panel A) and GGTase I (panel B) with the hydrophobicity of the peptide C-terminal residue. The values of k_{cat}/K_M are taken from Tables 1 and 2. Peptides with k_{cat}/K_M values below the detection limit were excluded from this plot. The $\Delta\Delta G^{\ddagger}$[2] values are plotted as a function of the $\Delta G°_{transfer}$ of the peptide X-residue (*46*) and fit to two lines. For FTase, the corresponding slopes of the lines are 2.0 ($R = 0.97$) (Q, S, A, T, Y, V) (◆) and 2.0 ($R = 0.70$) (M, C, F) (△). For GGTase I, the corresponding slopes of the lines are −2.0 ($R = 0.999$) (V, C, I, F) (●) and −1.8 ($R = 0.92$) (Y, M, L) (□).

[2] Calculated as follows: $\Delta\Delta G_{dissoc} = \Delta G_{TKCVIX} - \Delta G_{TKCVIM} = RT \ln K_D^{TKCVIM} - RT \ln K_D^{TKCVIX}$; $\Delta\Delta G^{\ddagger} = \Delta G^{\ddagger}_{TKCVIX} - \Delta G^{\ddagger}_{TKCVIM} = RT \ln k_{cat}/K_M^{TKCVIM} - RT \ln k_{cat}/K_M^{TKCVIX}$ (assuming that the [peptide] is 1 M); and $\Delta\Delta G^{\ddagger}(k_{chem}) = RT \ln k_{chem}^{TKCVIM} - RT \ln k_{chem}^{TKCVIX}$.

Although the binding affinities vary 10−30-fold for FTase and GGTase I as the C-terminal residue of K-Ras4B is modulated, there is little or no correlation of the $\Delta\Delta G_{dissoc}$ values with the hydrophobicity of the peptide X-group ($\Delta G°_{transfer}$) [data not shown, $R = 0.3$ (GGTase I) and 0.6 (FTase)]. These data indicate that substrate binding affinity has little dependence on the hydrophobicity of the X-residue side chain for uncharged amino acids.

The $\Delta\Delta G^{‡}$ values (calculated from $k_{cat}/K_M^{peptide}$) increase for FTase (Figure 4A) and, in contrast, decrease for GGTase I (Figure 4B) as the hydrophobicity of the C-terminal X-residue ($\Delta G°_{transfer}$) increases. However, the data suggest that the X-groups fall into at least two groups. For FTase, the $\Delta\Delta G^{‡}$ values for the peptides with the highest affinities (M, C, and F) can be described by one line (Figure 4A, slope = 2, $R = 0.7$). The $\Delta\Delta G^{‡}$ for the remaining peptides, with the exception of N at the X-position, can be described by a second line (Figure 4A, slope = 2, $R = 0.97$), indicating a significant increase in reactivity with decreasing hydrophobicity in both cases. However, the fact that the reactivity of the peptides cannot be described by a single line demonstrates that the structure of the X-group also affects reactivity; the side chains of M, C, and F confer a higher value of $k_{cat}/K_M^{peptide}$ than predicted solely from the hydrophobicity while the N side chain at the X-position has a lower activity than predicted. Reactivity ($\Delta\Delta G^{‡}$) of peptide substrates with FTase also correlates with volume of the X-group side chain ($-RT$ ln volume). In this case, linear correlations between reactivity and volume also split into multiple groups according to the X-group, as follows: Y, F, M, and Q ($R = 0.91$); V, T, N, and C ($R = 0.94$). The two smallest X-groups (A and S) have higher activity than predicted solely from the volume of the side chain. For GGTase I, the dependence of $\Delta\Delta G^{‡}$ (k_{cat}/K_M) on $\Delta G°_{transfer}$ can also be described by two, parallel lines (Figure 4B), including the following side chains at the X-position of the peptide substrate: V, C, F, and I (slope = −2, $R = 0.999$) and Y, M, and L (slope = −1.8, $R = 0.92$). For GGTase I, a modest correlation between reactivity ($\Delta\Delta G^{‡}$, k_{cat}/K_M) and side chain volume ($-RT$ ln volume) is observed for peptides with the following X-groups: Y, F, I, M, and L ($R = 0.73$). These data demonstrate that side chain hydrophobicity and structure are important for determining the substrate selectivity of FTase and GGTase I.

Furthermore, a correlation with $\Delta G°_{transfer}$ is observed for the $\Delta\Delta G^{‡}$ values calculated from k_{chem} measured for the reaction of FTase with these peptides; however, the slope is decreased. The values of $\Delta\Delta G^{‡}$ $(k_{chem})^2$ for reaction of FTase with peptides containing a terminal Q, S, A, T, Y, V, I, L, and F show a linear correlation with $\Delta G°_{transfer}$ (slope = 0.9, $R = 0.92$). The single turnover reactivity of FTase also correlates modestly with decreasing volume of the X-residue side chain (data not shown). For GGTase I, the dependence of $\Delta\Delta G^{‡}$ (k_{chem}) on $\Delta G°_{transfer}$ is less clear. The peptides appear to split into two groups: higher activity including X = F, L, M, V, T, and N (slope = −0.33, $R = 0.9$) and lower activity including X = I, C, Y, A, S, and Q (slope = −0.37, $R = 0.78$). Similarly, for GGTase I a modest correlation between $\Delta\Delta G^{‡}$ (k_{chem}) and increasing volume of the terminal amino acid is observed ($R = 0.6$).

The observation of two lines for the dependence of activity on the hydrophobicity of the X-group side chain (Figure 4) could be consistent with multiple X-residue binding sites. Two binding sites for the X-residue of peptides bound to FTase have been observed by structural studies (*36*). Crystallographic models indicate that the size and properties of the X-residue can shift the peptide backbone as well as the X-residue binding pocket (*12*). These changes in the orientation of the substrate in the active site likely lead to the observed alterations in activity, perhaps by altering the concentration of the reactive conformation of the prenyl diphosphate.

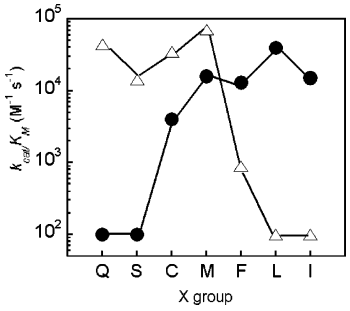

FIGURE 5: Differential reactivities of FTase and GGTase I. The multiple turnover rate constant, k_{cat}/K_M, was determined for FTase and GGTase I with dns-TKCVIX as described under Experimental Procedures and in the legend of Figure 4.

Peptides containing M, A, Q, and S at the C-terminus have been proposed to specify farnesylation catalyzed by FTase (*19*−*24*). The data presented here suggest that CaaX peptides containing C-terminal C, N, F, and T may also be efficiently farnesylated by FTase. Additionally, peptides containing leucine and phenylalanine in the X-position of the CaaX motif are proposed to specify geranylgeranylation catalyzed by GGTase I (*19*−*24*). Our data demonstrate that substrates with the X-residues M and I can also be efficient substrates of GGTase I while peptides with C-terminal V, C, and Y are potential substrates as well (Table 2). Moreover, the efficient binding and reactivity of TKCVIM and TKCVIF by both FTase and GGTase I observed in this study suggest that the dual specificity between FTase and GGTase I is due, at least in part, to the identity of the X-residue.

DISCUSSION

Role of the X-Residue in Specificity. We examined the functional importance of the C-terminal X-residue of the peptide substrate in the reactions catalyzed by FTase and GGTase I. The consistently high affinity of FTase and GGTase I for peptide substrates with various C-terminal residues is unexpected given the reported in vivo preferences of the enzymes for proteins containing enzyme-specific C-terminal residues (i.e., L and F for GGTase I and M, S, A, and Q for FTase). In contrast, the reactivity of peptides with FTase and GGTase I, reflected by k_{chem} and k_{cat}/K_M, in general correlates with the hydrophobicity and/or volume of the C-terminal amino acid of the peptide; transient and steady-state rate constants decrease for FTase and increase for GGTase I as the hydrophobicity or volume of the C-terminal X-residue increases (Figures 4 and 5). These results demonstrate that the primary determinant of substrate specificity in both FTase and GGTase I is reactivity, as opposed to substrate affinity. Kinetic versus thermodynamic specificity has previously been well documented for a

number of other enzymes, including the aminoacyl tRNA synthetases (*43*).

In FTase, the steady-state parameter $k_{cat}/K_M^{peptide}$ includes the rate constants for the steps from peptide binding to E·FPP through farnesylation (Scheme 1), including a step in which the prenyl chain of FPP rotates to position the C1 of FPP near the sulfur nucleophile in the peptide, as suggested by crystallographic data (*10*−*12*). Therefore, the value of $k_{cat}/K_M^{peptide}$ could be modulated by alterations in the rate constants for peptide association/dissociation, prenyl chain rotation, and/or the farnesylation step (Scheme 1). The data demonstrate that the identity of the X-group amino acid alters the rate constant of the prenylation step for both FTase and GGTase I; however, at least one other kinetic step must also be altered since the X-group side chain has a larger effect on the value of $k_{cat}/K_M^{peptide}$ compared to k_{chem} (Tables 1 and 2).

Under steady-state turnover, kinetic steps that occur after the first irreversible step should not affect the substrate selectivity (as determined by $k_{cat}/K_M^{peptide}$). For FTase and GGTase I, diphosphate dissociation is rapid and irreversible (*32*); therefore, the rate constant for dissociation of the prenylated peptide product would not be predicted to affect the peptide selectivity of these enzymes. Nonetheless, the hydrophobicity of the X-group has a similar effect on the rate constants for both product dissociation and farnesylation. This correlation may reflect similar interactions between the protein binding pocket and the X-group in the reactive ternary substrate complex and the product complex. In some cases, the product dissociation rate constant for prenylated peptides is so slow that only a single turnover occurs and the E·F-peptide product builds up (class B peptides). In this extreme case, slow product dissociation is a second mechanism used by these enzymes to determine substrate selectivity. Intriguingly, the dissociation of the F-peptide product can be accelerated by the addition of a second peptide substrate, rather than with FPP (*45*), potentially suggesting a novel mechanism for coordinating prenylation of pairs of protein substrates. These findings indicate that the properties of the X-residue may also affect the kinetics and thermodynamics of the movement of the prenylated product into the exit groove prior to product dissociation.

Differential X-Residue Binding Pockets. The structural determinants of the differences in FTase and GGTase I peptide specificity are presumably mainly localized to contacts with the X-residue in the binding pockets of these enzymes. However, the sequences of these pockets have significant homology, except that Ala98β, Trp102β, and Pro152β in the FTase structure are replaced with the more polar residues Thr45β, Thr49β, and Met 124β, respectively, in the GGTase I structure (Figure 1) (*11*, *27*). The different nature of these pockets is initially surprising since FTase reacts more readily with substrates containing more polar X-groups while GGTase I reacts more readily with substrates containing more nonpolar X-groups. However, the X-groups alter reactivity and not affinity. For FTase, the X-residue of the peptide substrate forms both van der Waals and electrostatic interactions with the enzyme (*36*). Subsites within the X-residue binding pocket of FTase possess hydrogen bond donating and accepting properties, thereby favorably accommodating most polar X-residues (*36*). For GGTase I, the peptide binding pocket stabilizes the X-residue side chain via van der Waals and hydrophobic interactions; thus, the hydrophobic character of the binding pocket discriminates against polar and charged side chains (*36*). Molecular modeling of the X-residue binding pockets of both FTase and GGTase I reveals that large, bulky amino acids as well as charged X-residues clash with the binding site and cause shifts in the peptide backbone (*36*). Moreover, these data reveal two possible X-residue binding sites for FTase: one site binds M, Q, and S while a second site was observed for F. Two binding sites have not been observed crystallographically for GGTase I (X = L, M, F), although alternative sites may exist for other amino acids (*36*). The data presented in Figure 4 are consistent with the observation of two binding sites for GGTase I as well as for FTase. However, even for FTase the X-groups that fall into the two binding sites (X = M, Q, S versus F) do not match the two groups identified by reactivity (Figure 4A). These discrepancies may reflect differences in conformation between inactive and reactive ternary complexes.

The identity of the X-residue side chain affects both the position of the residue in the binding pocket (Figure 1) and the conformation of the backbone of the peptide substrate in the active site of FTase and GGTase I (*36*). As such, the X-residue may affect the equilibrium between the active and inactive forms of the FPP/GGPP substrate as the carbon-1 of FPP/GGPP moves from the inactive form toward the cysteine sulfur of the peptide substrate to establish the active conformation and react (*10*−*12*). The size and polarity of the X-residue binding pocket may modulate reactivity by differentially orienting the protein/peptide substrate in the active site, thus encouraging or preventing side chain specific interactions that optimally induce the respective rotations about the carbon-1 of FPP/GGPP during the formation of the active ternary complex. The detailed structure of this proposed reactive ternary complex has thus far remained elusive yet holds valuable clues regarding the substrate specificities of these enzymes.

Role of the X-Residue in Vivo. The inverse relationship between hydrophobicity and reactivity for FTase and GGTase I leads to a group of substrates with reasonable reactivity for both enzymes (Figure 5, Tables 1 and 2). The identity of the X-group amino acid can specify for reactivity with either or both prenyltransferases. The overlapping substrate specificities of FTase and GGTase I may allow GGTase I to compensate for FTase when FTase-catalyzed prenylation becomes slow or inhibited, as observed previously with K-Ras4B (*18*). FTase-catalyzed prenylation is most obviously slowed in the presence of FTase inhibitors or when Mg(II) concentrations are low; however, farnesylation kinetics can also be affected by the properties of the protein substrate (*47*, companion paper).

The prenyl modification aids membrane association and protein−protein interactions that are essential for proper functioning of the modified protein in cellular signaling and regulatory events occurring at or near cellular membranes (*2*). The significance, if any, of a farnesyl versus a geranylgeranyl modification in vivo is not clear. A variety of data suggest that, for most substrates, the farnesyl versus geranylgeranyl distinction does not appear to be important for membrane association, at least at the plasma membrane (*18*, *48*−*50*). Localization of prenylated proteins to the peroxisomes, Golgi, and, perhaps, other specific organelles

may show a higher dependence on the structure of the prenyl group (*2*, *51*, *52*). Therefore, although the properties of the C-terminal residue of the peptide substrate affect reactivity with FTase and GGTase I, it is not yet clear whether the nature of the prenyl group causes differential behavior in vivo, such as targeting to a specific membrane. Moreover, the overlapping specificity between the enzymes hints at the importance of modifying substrates with a range of features, suggesting that in some cases the farnesyl versus geranylgeranyl distinction is not important.

ACKNOWLEDGMENT

We thank Andrea Stoddard for construction of the A197C PBP plasmid as well as June Pais for the development of the MDCC-labeled PBP assay. We also thank Professor Robert Coates for providing the 3-aza-GGPP used in these studies and Professor H. Peter Spielmann for careful reading of the manuscript and helpful suggestions.

REFERENCES

1. Yokoyama, K., Goodwin, G. W., Ghomashchi, F., and Gelb, M. H. (1992) Protein prenyltransferases, *Biochem. Soc. Trans. 20*, 489−494.
2. Zhang, F. L., and Casey, P. J. (1996) Protein prenylation: molecular mechanisms and functional consequences, *Annu. Rev. Biochem. 65*, 241−269.
3. Casey, P. J. (1994) Lipid modifications of G proteins, *Curr. Opin. Cell Biol. 6*, 219−225.
4. Marshall, C. J. (1993) Protein prenylation: a mediator of protein−protein interactions, *Science 259*, 1865−1866.
5. Reiss, Y., Brown, M. S., and Goldstein, J. L. (1992) Divalent cation and prenyl pyrophosphate specificities of the protein farnesyltransferase from rat brain, a zinc metalloenzyme, *J. Biol. Chem. 267*, 6403−6408.
6. Huang, C. C., Casey, P. J., and Fierke, C. A. (1997) Evidence for a catalytic role of zinc in protein farnesyltransferase. Spectroscopy of Co^{2+}-farnesyltransferase indicates metal coordination of the substrate thiolate, *J. Biol. Chem. 272*, 20−23.
7. Moomaw, J. F., and Casey, P. J. (1992) Mammalian protein geranylgeranyltransferase. Subunit composition and metal requirements, *J. Biol. Chem. 267*, 17438−17443.
8. Hightower, K. E., Huang, C. C., and Fierke, C. A. (1998) H-Ras peptide and protein substrates bind protein farnesyltransferase as an ionized thiolate, *Biochemistry 37*, 15555−15562.
9. Huang, C. C., Hightower, K. E., and Fierke, C. A. (2000) Mechanistic studies of rat protein farnesyltransferase indicate an associative transition state, *Biochemistry 39*, 2593−2602.
10. Long, S. B., Casey, P. J., and Beese, L. S. (2002) Reaction path of protein farnesyltransferase at atomic resolution, *Nature 419*, 645−650.
11. Taylor, J. S., Reid, T. S., Terry, K. L., and Beese, L. S. (2003) Structure of mammalian protein geranylgeranyltransferase type-I, *EMBO J. 22*, 5963−5974.
12. Pickett, J. S., Bowers, K. E., Hartman, H. L., Fu, H. W., Embry, A. C., and Fierke, C. A. (2003) Kinetic studies of protein farnesyltransferase mutants establish active substrate conformation, *Biochemistry 42*, 9741−9748.
13. Saderholm, M. J., Hightower, K. E., and Fierke, C. A. (2000) Role of metals in the reaction catalyzed by protein farnesyltransferase, *Biochemistry 39*, 12398−12405.
14. Bowers, K. E., and Fierke, C. A. (2004) Positively charged side chains in protein farnesyltransferase enhance catalysis by stabilizing the formation of the diphosphate leaving group, *Biochemistry 43*, 5256−5265.
15. Hartman, H. L., Bowers, K. E., and Fierke C. A. (2004) Lysine beta 311 of protein geranylgeranyltransferase type I partially replaces magnesium, *J. Biol. Chem. 279*, 30546−30553.
16. Bergo, M. O., Lieu, H. D., Gavino, B. J., Ambroziak, P., Otto, J. C., Casey, P. J., and Young, S. G. (2004) On the physiological importance of endoproteolysis of CAAX proteins: heart-specific RCE1 knockout mice develop a lethal cardiomyopathy, *J. Biol. Chem. 279*, 4729−4736.
17. Head, J. E., and Johnston, S. R. (2003) Protein farnesyltransferase inhibitors, *Expert Opin. Emerging Drugs 8*, 163−178.
18. Sebti, S. M., and Hamilton, A. D. (2001) Farnesyltransferase and geranylgeranyltransferase I inhibitors as novel agents for cancer and cardiovascular diseases, *Farnesyltransferase Inhib. Cancer Ther.*, 197−219.
19. Casey, P. J., Thissen, J. A., and Moomaw, J. F. (1991) Enzymatic modification of proteins with a geranylgeranyl isoprenoid, *Proc. Natl. Acad. Sci. U.S.A. 88*, 8631−8635.
20. Yokoyama, K., Goodwin, G. W., Ghomashchi, F., and Gelb, M. H. (1991) A protein geranylgeranyltransferase from bovine brain: implications for protein prenylation specificity, *Proc. Natl. Acad. Sci. U.S.A. 88*, 5302−5306.
21. Moores, S. L., Schaber, M. D., Mosser, S. D., Rands, E., O'Hara, M. B., Garsky, V. M., Marshall, M. S., and Gibbs, J. B. (1991) Sequence dependence of protein isoprenylation, *J. Biol. Chem. 266*, 14603−14610.
22. Reiss, Y., Seabra, M. C., Armstrong, S. A., Slaughter, C. A., and Brown, M. S. (1991) Nonidentical subunits of p21H-ras farnesyltransferase. Peptide binding and farnesyl pyrophosphate carrier functions, *J. Biol. Chem. 266*, 10672−10677.
23. Omer, C. A., Kral, A. M., Diehl, R. E., Prendergast, G. C., Powers, S., Allen, C. M., and Kohl, N. E. (1993) Characterization of recombinant human farnesyl-protein transferase: cloning, expression, farnesyl diphosphate binding, and functional homology with yeast prenyl-protein transferases, *Biochemistry 32*, 5167−5176.
24. Caplin, B. E., Hettich, L. A., and Marshall, M. S. (1994) Substrate characterization of the *Saccharomyces cerevisiae* protein farnesyltransferase and type-I protein geranylgeranyltransferase, *Biochim. Biophys. Acta 1205*, 39−48.
25. Cox, A. D., and Der, C. J. (1997) Farnesyltransferase inhibitors and cancer treatment: targeting simply Ras?, *Biochim. Biophys. Acta 1333*, 51−71.
26. Chen, Z., Sun, J., Pradines, A., Favre, G., and Sebti, S. M. (2000) Both farnesylated and geranylgeranylated RhoB inhibit malignant transformation and suppress human tumor growth in nude mice, *J. Biol. Chem. 275*, 17974−17978.
27. Long, S. B., Casey, P. J., and Beese, L. S. (2000) The basis for K-Ras4B binding specificity to protein farnesyltransferase revealed by 2 Å resolution ternary complex structures, *Structure 8*, 209−222.
28. Riddles, P. W., Blakeley, R. L., and Zerner, B. (1979) Ellman's reagent: 5,5′-dithiobis(2-nitrobenzoic acid)—a reexamination, *Anal. Biochem. 94*, 75−81.
29. Zimmerman, K. K., Scholten, J. D., Huang, C. C., and Hupe, D. J. (1998) High-level expression of rat farnesyl:protein transferase in *Escherichia coli* as a translationally coupled heterodimer, *Protein Expression Purif. 14*, 395−402.
30. Sagami, H., Korenaga, T., Ogura, K., Steiger, A., and Coates, R. M. (1992) Studies on geranylgeranyl diphosphate synthase from rat liver: specific inhibition by 3-azageranylgeranyl diphosphate, *Arch. Biochem. Biophys. 297*, 314−320.
31. Hirshberg, M., Henrick, K., Haire, L. L., Vasisht, N., Brune, M., and Webb, M. R. (1998) Crystal structure of phosphate binding protein labeled with a coumarin fluorophore, a probe for inorganic phosphate, *Biochemistry 37*, 10381−10385.
32. Pais, J. E., Bowers, K. E., Stoddard, A. K., and Fierke, C. A. (2005) A continuous fluorescent assay for protein prenyltransferases measuring diphosphate release, *Anal. Biochem. 345*, 302−311.
33. Pompliano, D. L., Gomez, R. P., and Anthony, N. J. (1992) Intramolecular fluorescence enhancement: a continuous assay of ras farnesyl:protein transferase, *J. Am. Chem. Soc. 114*, 7945−7946.
34. Cassidy, P. B., Dolence, J. M., and Poulter, C. D. (1995) Continuous fluorescence assay for protein farnesyltransferase, *Methods Enzymol. 250*, 30−43.
35. Chehade, K. A., Kiegiel, K., Isaacs, R. J., Pickett, J. S., Bowers, K. E., Fierke, C. A., and Spielmann, H. P. (2002) Photoaffinity analogues of farnesyl pyrophosphate transferable by protein farnesyl transferase, *J. Am. Chem. Soc. 124*, 8206−8219.
36. Reid, T. S., Terry, K. L., and Beese, L. S. (2004) Crystallographic analysis of CaaX prenyltransferases complexed with substrates defines rules of protein substrate selectivity, *J. Mol. Biol. 343*, 417−433.
37. Reiss, Y., Stradley, S. J., Gierasch, L. M., and Goldstein, J. L. (1991) Sequence requirement for peptide recognition by rat brain

p21ras protein farnesyltransferase, *Proc. Natl. Acad. Sci. U.S.A. 88*, 732−736.
38. Long, S. B., Hancock, P. J., Kral, A. M., and Beese, L. S. (2001) The crystal structure of human protein farnesyltransferase reveals the basis for inhibition by CaaX tetrapeptides and their mimetics, *Proc. Natl. Acad. Sci. U.S.A. 98*, 12948−12953.
39. Zhang, F. L., and Casey, P. J. (1996) Influence of metal ions on substrate binding and catalytic activity of mammalian protein geranylgeranyltransferase type-I, *Biochem. J. 320*, 925−932.
40. Pompliano, D. L., Schaber, M. D., Mosser, S. D., Omer, C. A., and Gibbs, J. B. (1993) Isoprenoid diphosphate utilization by recombinant human farnesyl:protein transferase: interactive binding between substrates and a preferred kinetic pathway, *Biochemistry 32*, 8341−8347.
41. Furfine, E. S., Leban, J. J., Landavazo, A., and Casey, P. J. (1995) Protein farnesyltransferase: kinetics of farnesyl pyrophosphate binding and product release, *Biochemistry 34*, 6857−6862.
42. Yokoyama, K., McGeady, P., and Gelb, M. H. (1995) Mammalian protein geranylgeranyltransferase-I: substrate specificity, kinetic mechanism, metal requirements, and affinity labeling, *Biochemistry 34*, 1344−1354.
43. Fersht, A. R. (1999) *Structure and Mechanism in Protein Science: A Guide to Enzyme Catalysis and Protein Folding*, W. H. Freeman, New York.
44. Yokoyama, K., Zimmerman, K., and Gelb, M. H. (1997) Differential prenyl pyrophosphate binding to mammalian protein geranylgeranyltransferase-I and protein farnesyltransferase and its consequence on the specificity of protein prenylation, *J. Biol. Chem. 272*, 3944−3952.
45. Tschantz, W. R., Zhang, L., and Casey, P. J. (1999) Cloning, expression, and cellular localization of a human prenylcysteine lyase, *J. Biol. Chem. 274*, 35802−35808.
46. Karplus, P. A. (1997) Hydrophobicity regained, *Protein Sci. 6*, 1302−1307.
47. Hicks, K. A., Hartman, H. L., and Fierke, C. A. (2005) Upstream polybasic region in peptides enhances dual specificity for prenylation by both farnesyltransferase and geranylgeranyltransferase type I, *Biochemistry 44*, 15325−15333.
48. Powers, S., Michaelis, S., Broek, D., Santa Anna, S., Field, J., and Wigler, M. (1986) RAM, a gene of yeast required for a functional modification of RAS proteins and for production of mating pheromone a-factor, *Cell 47*, 413−422.
49. Trueblood, C. E., Ohya, Y., and Rine, J. (1993) Genetic evidence for in vivo cross-specificity of the CaaX-box protein prenyltransferases farnesyltransferase and geranylgeranyltransferase-I in *Saccharomyces cerevisiae*, *Mol. Cell. Biol. 13*, 4260−4275.
50. Solski, P. A., Helms, W., Keely, P. J., and Der, C. J. (2002) RhoA biological activity is dependent on prenylation but independent of specific isoprenoid modification,*Cell Growth Differ. 13*, 363−373.
51. James, G. L., Goldstein, J. L., Pathak, R. K., and Brown, M. S. (1994) PxF, a prenylated protein of peroxisomes, *J. Biol. Chem. 269*, 14182−14190.
52. Beranger, F., Goud, B., and de Gunzburg, J. (1991) Association of the Ras-antagonistic Rap1/Krev-1 proteins with the Golgi complex, *Proc. Natl. Acad. Sci. U.S.A. 88*, 1606−1610.

BI0509503